Front. Earth Sci. 2016, 10(4): 772–783
DOI 10.1007/s11707-016-0559-2

RESEARCH ARTICLE

Multi-antenna synchronized global navigation satellite system receiver and its advantages in high-precision positioning applications

Danan DONG[1,2,3], Wen CHEN (✉)[1,2], Miaomiao CAI[1], Feng ZHOU[1], Minghua WANG[4], Chao YU[1,2], Zhengqi ZHENG[1], Yuanfei WANG[1,3]

1 Engineering Center of SHMEC for Space Information and GNSS, East China Normal University, Shanghai 200241, China
2 Shanghai Key Laboratory of Multidimensional Information Processing, East China Normal University, Shanghai 200241, China
3 Key Laboratory of Geographic Information Science, Ministry of Education, East China Normal University, Shanghai 200241, China
4 College of Surveying and Geo-informatics, Tongji University, Shanghai 200092, China

Abstract The multi-antenna synchronized global navigation satellite system receiver is a high precision, low cost, and widely used emerging receiver. Using this type of receiver, the satellite and receiver clock errors can be eliminated simultaneously by forming between antenna single-differences, which is equivalent to the conventional double-difference model. However, current multi-antenna synchronized global navigation satellite system receiver products have not fully realized their potential to achieve better accuracy, efficiency, and broader applications. This paper introduces the conceptual design and derivable products of multi-antenna synchronized global navigation satellite system receivers involving the aspects of attitude determination, multipath effect mitigation, phase center variation correction, and ground-based carrier phase wind-up calibration. Through case studies, the advantages of multi-antenna synchronized global navigation satellite system receivers in high-precision positioning applications are demonstrated.

Keywords multi-antenna synchronized global navigation satellite system receiver, high-precision positioning, attitude determination, multipath effect mitigation, phase center variation correction, ground-based carrier phase wind-up calibration

1 Introduction

As an emerging positioning and attitude determination approach in the past two decades, global positioning systems (GPS) have been widely used in automatic navigation of intelligent cars and spacecraft, shipping, deformation monitoring, and military devices such as radars, cannons, tanks, missiles, and shoulder launchers. The evolution of such a system can be traced back to the early 1980s.

In the early 1980s, GPS was applied to attitude determination to complement the weaknesses of inertial navigation systems, which included error accumulation, long cold starting time, complicated structure, and high cost. At this stage, these applications of GPS were confined to system simulations (Hermann, 1985) or military experiments (Kruczynski et al., 1989) because they performed relatively poorly and were expensive.

Since the 1990s, several big companies have conducted extensive studies and tests for the GPS attitude determination system, and launched several receivers and processing software. Such programs included the 3DF of Ashtech Inc. (Ashtech Inc., 1991) and the Tans Vector of Trimble Co. Ltd (Wilson and Tonnemacher, 1992). However, this specialized equipment was expensive and had poor flexibility in application. With the continuous progress and development of GPS receiver technology, manufacturers proposed a series of high-quality GPS original equipment manufacturer (OEM) boards (Fenton et al., 1991; Cannon et al., 1993). Subsequently, attitude measurement experiments combining multiple independent OEM boards were undertaken (Cannon and Lachapelle, 1992; Lu et al., 1994).

In recent years, to further reduce costs, OEM boards with clock synchronization technology (signals from multi-antennas are synchronized using a common clock) have been introduced for precise attitude determination. In

Received April 7, 2015; accepted August 25, 2015

E-mail: wchen@sist.ecnu.edu.cn

this study, this type of receiver system will be termed as the multi-antenna synchronized global navigation satellite system (MS-GNSS) receiver system. For simplicity, 'receiver system' will be replaced by 'receiver'. Compared with the multi-antenna receiver that combines two standalone devices, the MS-GNSS receiver ensures lower cost and greater accuracy when determining directional attitude.

Recently, commercial MS-GNSS receivers have expanded rapidly. Such equipment exhibits great advantages such as low cost, flexibility, and high precision. However, the benefits of the clock synchronization technology have not yet been fully realized. First, some commercial products of this type of receiver still adopt the double-difference (DD) algorithm. Second, the MS-GNSS receiver is still limited in use to attitude determination. This study aims at investigating the potential of the MS-GNSS receiver with a single-difference (SD) algorithm to further improve its accuracy and flexibility and to extend its applications.

The rest of the article is structured as follows. An introduction to the MS-GNSS receiver, which includes its conceptual design and typical products, is provided in Section 2. The potential of this new type of receiver in high-precision positioning applications (such as attitude determination, multipath mitigation, phase center variation correction, and ground-based carrier phase wind-up calibration) is presented in Section 3. Section 4 concludes with a summary.

2 MS-GNSS receiver

2.1 Conceptual design

The conceptual design of a typical MS-GNSS receiver is shown in Fig. 1 (taking a dual-antenna device as an example). The signal processing workflow is as follows: First, the radio frequency (RF) signals are received by the master and slave antennas. Next, a common reference clock is used to convert the RF signals into intermediate frequency (IF) signals. The IF signals are then correlated with the locally generated pseudo-random code to obtain raw observations such as pseudo-range, carrier phase, signal-to-noise ratio, and Doppler. Finally, the position, time, and attitude solutions are computed in the central processing unit based on the measurements mentioned above. A critical feature of this emerging receiver is that all the tracking channels of the multiple antennas are controlled by a single oscillator.

2.2 Typical products

Typical commercial products of the MS-GNSS receiver and their basic parameters are presented in Table 1.

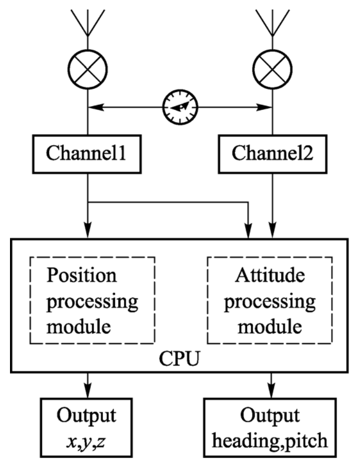

Fig. 1 Conceptual design of the MS-GNSS receiver.

Table 1 Typical MS-GNSS receivers

Receiver	Company	Number of antennas	Satellite
AsteRx2eH	Septentrio NV	2	GPS, GLONASS
BD982	Trimble	2	GPS, GLONASS, BeiDou, SBAS
Triumph-4x	Javad	4	GPS, GLONASS, SBAS
TOAS100D	OlinkStar	2	GPS, BeiDou
K528	ComNav	2	GPS, BeiDou

3 Advantages of the MS-GNSS receiver in high-precision positioning applications

This section explains the advantages of the MS-GNSS receiver in high-precision positioning applications such as attitude determination, multipath mitigation, antenna phase center variation correction, and ground-based carrier phase wind-up calibration.

3.1 Attitude determination

Attitude determination is the most important application of multi-antenna GNSS systems. Its calculation process is divided into two steps. The first is to solve for the baseline vector using carrier phase observations, the second is to obtain the carrier attitude from the baseline vector. The carrier phase observation from a single antenna is defined as:

$$\phi_A = \frac{1}{\lambda}\left(\rho_A^i + c\cdot\delta\tau_{r_A} - c\cdot\delta\tau_s^i + T_A^i + I_A^i\right) + N_A^i + \varphi_{PCV_A} + \varphi_{UPD_A} + \varphi_{MP_A}^i + \varepsilon, \tag{1}$$

where i is the satellite index; A is the index of the receiving antenna; ρ is the geometric distance; $\delta\tau_r$ and $\delta\tau_s$ are the receiver and satellite clock errors; T and I are the troposphere and ionosphere delays, where T is frequency independent and I is proportional to the inverse of frequency squares; N is the ambiguity; φ_{PCV} is the antenna phase center variation; φ_{UPD} is the uncalibrated phase delay (UPD), which is satellite independent (Ge et al., 2008); φ_{MP} is the multipath error; λ is the wavelength of the carrier phase electromagnetic wave; c is the velocity of light; and ε are the measurement noise and unmodelled errors, such as the orbital error.

For between-antenna SD observables, the satellite clock term is canceled out. For the MS-GNSS receiver, the receiver clock term is further canceled out because of the common clock. For short baseline observables, the atmospheric and ionospheric delays, and other geophysical delays (such as from earth tide) are greatly reduced and can be ignored. If we set up the orientation of the two antennas to be the same, the receiver antenna phase center variation term is also eliminated. Thus, the SD observation equation becomes:

$$\Delta\phi = \frac{1}{\lambda}\Delta\rho_{AB}^{i} + \Delta N_{AB}^{i} + \Delta\varphi_{UPD_{AB}} + \Delta\varphi_{MP_{AB}}^{i} + \Delta\varepsilon_{AB}, \quad (2)$$

where Δ is the SD operator between the master antenna B and the slave antenna A.

For comparison, we also list the DD carrier phase observation equation:

$$\nabla\Delta\phi = \frac{1}{\lambda}\nabla\Delta\rho_{AB}^{ij} + \nabla\Delta N_{AB}^{ij} + \nabla\Delta\varphi_{MPAB}^{ij} + \nabla\Delta\varepsilon_{AB}, \quad (3)$$

where$\nabla\Delta$ is the DD operator between antennas and satellites.

Because the DD model can eliminate satellite and receiver clock errors simultaneously, it is widely used in commercial receivers. Although the SD model can also remove both satellite and receiver clock errors for the MS-GNSS receiver, which is functionally equivalent to the DD model, many companies still adopt the DD model for its maturity. Another reason the DD model is preferred is that the integer ambiguity term and the float UPD term are fully coupled in the SD model. Thus, its ambiguity term lost its integer nature and the integer ambiguity resolving algorithm, such as the LAMBDA algorithm (Teunissen, 1995; Teunissen et al., 1997), cannot be directly implemented. However, the SD model has many potential advantages and broad use. For example, the DD model can only obtain the between satellite differenced baseline multipath and phase center variation solutions, while the SD model obtains them for each satellite. Thus, the SD model can easily construct the baseline multipath and phase center variation correction model for real-time applications. Details will be discussed in the following sections.

3.1.1 A new approach for integer ambiguity resolution of SD observables

For the MS-GNSS receiver, both the satellite clock and receiver clock errors can be eliminated simultaneously by forming SD (denoted by MS-SD in this study). Compared with the DD algorithm, the MS-SD model has more observations and redundancy and lower correlations among estimated parameters. Taking the dual-frequency receivers as an example, the theoretical performance comparison between the DD and MS-SD algorithm is presented in Table 2 where n is the number of satellites and m is the number of epochs.

Table 2 Theoretical performance comparison between DD and MS-SD algorithm

	DD	MS-SD
Number of observations	$(n-1)*m*4$	$n*m*4$
Redundancy	$(n-1)*m*4-(n-1)*2-6$	$n*m*4-n*2-8$
Correlation	High	Low

The biggest obstacle to realizing the MS-SD algorithm is the resolution of the integer ambiguity. Only in the DD case is the ambiguity purely integer. Currently, the widely used LAMBDA algorithm (Teunissen,1995; Teunissen et al.,1997) to solve integer ambiguity first de-correlates the ambiguities by means of the Z-transformation, and then obtains integer ambiguity by searching over an ellipsoidal ambiguity search space. Since this procedure is based on the premise that the initial real phase must be eliminated, it is viable for fixing the DD integer ambiguity.

To resolve the difficulty in the MS-SD case of fixing the integer ambiguities contaminated by the float UPD (or line biases), Li et al. (2004) proposed a new algorithm integrating both the MS-SD and DD models. The proposed algorithm is composed of two key steps. The first step is to fix integer ambiguities in the DD carrier phase combinations, and the second step is to solve UPD and MS-SD integer ambiguity from MS-SD observations based on the coarse attitude obtained from the DD model. The average values of the bias between this GPS and inertial measurement unit solutions on roll, pitch, and yaw are 0.012°, –0.056°, and –0.054°, respectively, and the standard deviations are 0.16°, 0.13°, and 0.23°.

Dong et al. (2015a) and Zhou et al. (2015) proposed a new ambiguity substitution approach (ASA) for the MS-SD model for real-time attitude determination. The ASA method introduces an additional UPD parameter estimated together with the ambiguity parameters. Such a procedure functionally raises correlations between the ambiguity parameters, contrasting with the de-correlation philosophy of the LAMBDA algorithm (Teunissen,1995; Teunissen et al.,1997). The ASA approach successfully separates the common real initial phase from integer ambiguity because of the strong correlation between this additive parameter and the ambiguity parameters. This method solves the MS-SD integer ambiguity with improved efficiency and accuracy, which makes the advanced SD model feasible with full use of clock synchronization technology. To test the accuracy of the MS-SD method, a comparative experiment of dynamic short baseline attitude determinations with the Trimble software was conducted based on a turning table (Fig. 2(a)). In this experiment, a Trimble BD982 MS-GNSS receiver was used. Two antennas were connected to the same receiver and mounted on a turning table. The turning table rotated clockwise and counter-clockwise to 325° alternately. The above process was repeated for 31 cycles. The baseline was 0.175 m long. The sampling frequency was 10 Hz. We solved the baseline vector parameters in the geographic coordinate system using the Kalman filtering algorithm, where the x-axis was towards the east and the y-axis towards the north. Fig. 2(b) shows the trajectories of the estimated baseline vector between the master and slave antennas. The red symbols represent the results of the MS-SD method while the blue symbols represent the output of the Trimble software. It indicates that the trajectory obtained by the proposed method is consistent with the results from the Trimble software, and the results of the former method display lower dispersion.

3.1.2 Integrated attitude determination with GPS/GLONASS

Satellite visibility is a major concern in an urban environment. A joint solution of multi-satellite systems is an effective strategy for this problem. GLONASS is an important component of GNSS. However, the DD model cannot be used directly because the GLONASS signals are of different frequencies. Keong and Lachapelle (2000) developed a MS-SD model to determine heading and pitch using GPS/GLONASS signals. To eliminate the receiver clock error, a common oscillator was connected to two Ashtech GG24™ receivers (Fig. 3). A kinematic test was carried out to compare the performance of the GPS/GNOLASS SD and GPS DD solutions. The results indicate that the availability of the former solution is 8% higher than of the latter. Thus, with the help of multi-antenna synchronization technology, the GPS/GLONASS SD model shows potential to improve availability under signal masking conditions.

3.2 Multipath effect mitigation

The multipath effect remains an unsolved error source that complicates high-precision GPS analysis. In addition to direct signals from the satellite, a GPS receiver simultaneously receives reflected signals from surrounding reflectors. The multipath effect cannot be estimated through the difference technique or analytic model because of the irregular shape, distribution, and complicated reflective properties of reflecting objects. Therefore, researchers have proposed various approaches for multipath effect mitigation. These approaches include: 1) Selecting a proper site to avoid strong reflection and intense radiation, 2) Improving GPS receiver hardware by modifying the antenna structure (Young and Meehan, 1988) and the tracking loop technologies (Nee, 1992; Van Dierendonck et al., 1992; Townsend and Fenton, 1994), and 3) Several types of data processing methods. The site selection approaches are subjected to real environments and receiver hardware improvement technologies, which partially reduce multipath errors but increase costs.

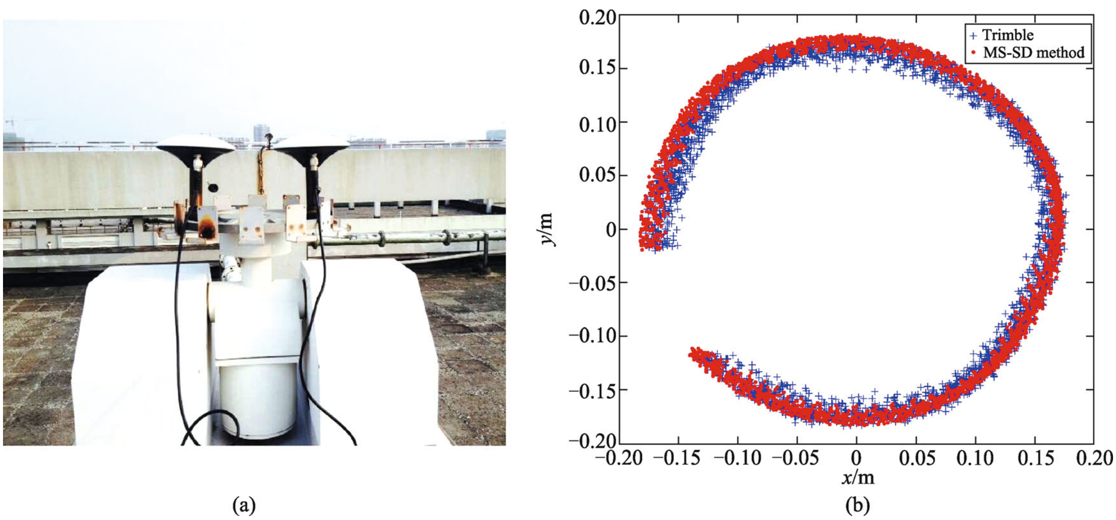

Fig. 2 Comparative experiment between MS-SD method and Trimble software. (a) Dynamic short baseline attitude determination experiment based on turning table. (b) The estimated trajectories of baseline vectors between the master and slave antennas using MS-SD method and Trimble software.

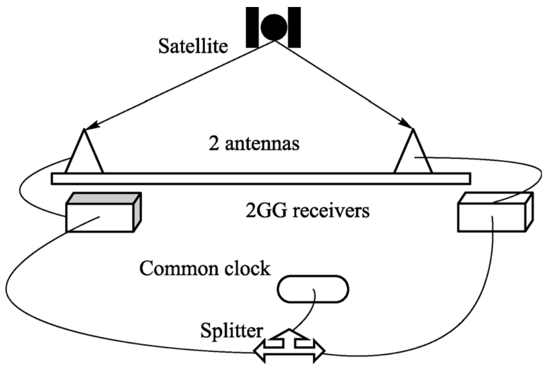

Fig. 3 Hardware Installation for GPS/GNONASS system (Keong and Lachapelle, 2000).

Software-based data processing methods become the main means of mitigating multipath errors. These methods can be divided into two categories. One is offline data processing methods such as wavelet analysis (Souza and Monico, 2004) and filtering methods for separating random and multipath errors (Ge et al., 2000; Zheng et al., 2005). The other is using real-time processing algorithms including the sidereal filtering method based on the temporal repeated nature of multipaths for the satellite constellation (Genrich and Bock, 1992; Bock et al., 2000; Ragheb et al., 2007) and the look-up table method based on the repeatability between multipath and the satellite position in the sky (Cohen and Parkinson, 1991; Dong et al., 2014; Fuhrmann et al., 2015). The benefits of using MS-GNSS receivers for solving multipath errors in real time will be discussed in detail in the next two sections.

3.2.1 Sidereal filtering

Sidereal filtering is developed on the basis that the GPS satellite constellation in the sky repeats nearly every sidereal day (23 h 56 m 04 s). If the receiving antenna is in a fixed position and the surrounding environment remains static, the relative geometric relationship of the satellite-to-antenna phase center is the same each sidereal day, and the multipath error of the observation site will also repeat. Taking advantage of this property, the repetitive multipath noise can be eliminated by modeling the repeated observations on consecutive sidereal days. However, some studies show that each GPS satellite has a different orbital repeat period (Choi et al., 2004; Larson et al., 2007), which will affect the accuracy of sidereal filtering especially when processing real-time estimations. For this reason, some advanced sidereal filtering algorithms have been explored in recent studies, for instance, the modified sidereal filtering (Choi et al., 2004) and the aspect repeat time adjustment (ARTA) method (Larson et al., 2007).

The ARTA method is more consistent with the real GPS orbits, and can improve the accuracy of GPS positioning with a high sample rate. However, this method is suitable only when the visible satellites are the same on each day (Bilich, 2006; Larson et al., 2007), which is difficult to satisfy in reality. To solve the above problem, Zhong et al. (2010) proposed a new sidereal filtering algorithm based on SD. Experiments were conducted to compare the suggested method with classical sidereal filtering and ARTA. The results show that this method can reduce the root mean square value of 3D GPS positioning noises by 82% on average and improve the accuracy of the sidereal filtering and ARTA method by 13% and 7% respectively. Ye et al. (2014) applied a similar approach to BeiDou satellite observations. The experimental results showed that the proposed approach can promote the precision of BeiDou positioning by 56%, 48%, and 48% in the north, east, and vertical components. By using combined GPS + BD positioning, the accuracy can reach 0.95 mm, 0.92 mm, and 2.31 mm in the three directions respectively, which is better than that of the single system.

Because the MS-GNSS receivers were not used in the above studies, to eliminate receiver clock error the DD residuals were first obtained by forming DD, and were then transferred to the SD residuals for subsequent calculations. Suppose ε_{AB}^{i} is the SD residual of receiver A and B with satellite i and ε_{AB}^{ij} is the DD residual of receiver A and B with satellite i and j, the transformation matrix is as follows:

$$\begin{bmatrix} w_1 & w_2 & w_3 & \cdots & w_n \\ 1 & -1 & 0 & \cdots & 0 \\ 1 & 0 & -1 & \cdots & 0 \\ & & \ddots & & \\ 1 & 0 & 0 & \cdots & -1 \end{bmatrix} \begin{bmatrix} \varepsilon_{AB}^{1} \\ \varepsilon_{AB}^{2} \\ \varepsilon_{AB}^{3} \\ \vdots \\ \varepsilon_{AB}^{n} \end{bmatrix} = \begin{bmatrix} \sum w_i \varepsilon_{AB}^{i} \\ \varepsilon_{AB}^{12} \\ \varepsilon_{AB}^{13} \\ \vdots \\ \varepsilon_{AB}^{1n} \end{bmatrix}, \quad (4)$$

where w_i is the weighting factor for each satellite. If there are n single differences, only $n-1$ linearly independent DDs can be formed. To obtain the inverse matrix, the "zero mean" assumption (Alber et al., 2000), which set $\sum w_i \varepsilon_{AB}^{i} = 0$, can be used to derive the weighting factor w_i.

As mentioned in Alber et al. (2000), the "zero mean" constraint will introduce extra errors during the transformation process. Suppose there are five satellites, and their weighting factors are equal. Based on the "zero mean" constraint, Eq. (4) can be expressed as:

$$\begin{bmatrix} 1 & 1 & 1 & 1 & 1 \\ 1 & -1 & 0 & 0 & 0 \\ 1 & 0 & -1 & 0 & 0 \\ 1 & 0 & 0 & -1 & 0 \\ 1 & 0 & 0 & 0 & -1 \end{bmatrix} \begin{bmatrix} \varepsilon_{AB}^{1} \\ \varepsilon_{AB}^{2} \\ \varepsilon_{AB}^{3} \\ \varepsilon_{AB}^{4} \\ \varepsilon_{AB}^{5} \end{bmatrix}_{est} = \begin{bmatrix} 0 \\ \varepsilon_{AB}^{12} \\ \varepsilon_{AB}^{13} \\ \varepsilon_{AB}^{14} \\ \varepsilon_{AB}^{15} \end{bmatrix}_{real} = \begin{bmatrix} 0 \\ \varepsilon_{AB}^{1}-\varepsilon_{AB}^{2} \\ \varepsilon_{AB}^{1}-\varepsilon_{AB}^{3} \\ \varepsilon_{AB}^{1}-\varepsilon_{AB}^{4} \\ \varepsilon_{AB}^{1}-\varepsilon_{AB}^{5} \end{bmatrix}_{real}, \tag{5}$$

and the SD residual becomes:

$$\begin{bmatrix} \varepsilon_{AB}^{1} \\ \varepsilon_{AB}^{2} \\ \varepsilon_{AB}^{3} \\ \varepsilon_{AB}^{4} \\ \varepsilon_{AB}^{5} \end{bmatrix}_{est} = \begin{bmatrix} \frac{1}{5} & \frac{1}{5} & \frac{1}{5} & \frac{1}{5} & \frac{1}{5} \\ \frac{1}{5} & -\frac{4}{5} & \frac{1}{5} & \frac{1}{5} & \frac{1}{5} \\ \frac{1}{5} & \frac{1}{5} & -\frac{4}{5} & \frac{1}{5} & \frac{1}{5} \\ \frac{1}{5} & \frac{1}{5} & \frac{1}{5} & -\frac{4}{5} & \frac{1}{5} \\ \frac{1}{5} & \frac{1}{5} & \frac{1}{5} & \frac{1}{5} & -\frac{4}{5} \end{bmatrix} \begin{bmatrix} 0 \\ \varepsilon_{AB}^{12} \\ \varepsilon_{AB}^{13} \\ \varepsilon_{AB}^{14} \\ \varepsilon_{AB}^{15} \end{bmatrix}_{real}$$

$$= \begin{bmatrix} \frac{4}{5}\varepsilon_{AB}^{1} - \frac{1}{5}(\varepsilon_{AB}^{2} + \varepsilon_{AB}^{3} + \varepsilon_{AB}^{4} + \varepsilon_{AB}^{5}) \\ \frac{4}{5}\varepsilon_{AB}^{2} - \frac{1}{5}(\varepsilon_{AB}^{1} + \varepsilon_{AB}^{3} + \varepsilon_{AB}^{4} + \varepsilon_{AB}^{5}) \\ \frac{4}{5}\varepsilon_{AB}^{3} - \frac{1}{5}(\varepsilon_{AB}^{2} + \varepsilon_{AB}^{1} + \varepsilon_{AB}^{4} + \varepsilon_{AB}^{5}) \\ \frac{4}{5}\varepsilon_{AB}^{4} - \frac{1}{5}(\varepsilon_{AB}^{2} + \varepsilon_{AB}^{3} + \varepsilon_{AB}^{1} + \varepsilon_{AB}^{5}) \\ \frac{4}{5}\varepsilon_{AB}^{5} - \frac{1}{5}(\varepsilon_{AB}^{2} + \varepsilon_{AB}^{3} + \varepsilon_{AB}^{4} + \varepsilon_{AB}^{1}) \end{bmatrix}_{real}. \tag{6}$$

Eq. (6) shows that the estimated SD residual is not the real SD residual, and these extra errors will subsequently cause estimation errors of the multipath effect.

However, with the MS-GNSS receiver, we can obtain the SD residuals directly and avoid the occurrence of transformation errors, which will then enhance the accuracy of the estimated multipath effect.

3.2.2 Look-up table method

Sidereal filtering is based on the time-domain repetitive geometric relationships between the satellite, receiving antenna, and surrounding environment. However, the look-up table method is based on the fact that the multipath effect is only related to the orbital position of the transmitting source in the sky under the premise of an unchanged relative position between the reflection source and the receiving antenna. Therefore, multipath effect corrections can be determined with the elevation and azimuth angles of the satellite by mapping the multipath environment around the GPS antenna (Cohen and Parkinson, 1991; Cohen, 1992). The advantage of the look-up table method is that it is independent of the satellite and explores the space-time invariance of the multipath effect under an unchanged environment. Therefore, this method is applicable for static environments and also for dynamic carriers where the dominant multipath environment is static, such as for ships and airplanes.

Relying on the MS-GNSS receiver, Dong et al. (2014) constructed a multipath hemispherical map (MHM) to mitigate the multipath effects. Because the receiver clock error is eliminated, the SD phase of the short baseline is expressed as:

$$\Delta\phi = \Delta\varphi_g^i + \Delta\varphi_{MP}^i + \Delta\varphi_{UPD} + \Delta\varepsilon, \tag{7}$$

where Δ is the MS-SD operator, i is the satellite index, ϕ is the observed carrier phase, φ_g is the geometry distance including the ambiguity parameter, φ_{MP} is the phase distortion caused by the multipath effect, φ_{UPD} is the UPD parameter, and ε is the residual error.

The geometry term in Eq. (7) can be eliminated by tightly constraining the baseline vector and resolving the integer ambiguities, and the gridded $\Delta\varphi_{MP}^i$ are then estimated directly. Although the solutions are constructed on the geocentric coordination system, the satellite position in the sky is determined by switching to the topocentric coordinate system (taking the master antenna as the origin). Then we can obtain the azimuth angle α and elevation angel z of satellite i:

$$\alpha = \tan^{-1}\left(\frac{E}{N}\right), \tag{8}$$

$$z = \tan^{-1}\left(\frac{U}{\sqrt{E^2 + N^2}}\right), \tag{9}$$

where N, E, U is the coordination of satellite i in the topocentric coordinate system. Thus, the gridded multipath of the short baseline $\Delta\varphi_{MP}^i$ can be visualized as a celestial hemispherical map of multipath errors, which is shown in Fig. 4. The multi-days multipath mitigation experimental results based on a static short baseline demonstrate that MHM is able to reduce the multipath error by more than 40%.

The look-up table method becomes feasible owing to the emergence of the MS-GNSS receiver. The applications of multipath mitigation are consequently extended to the

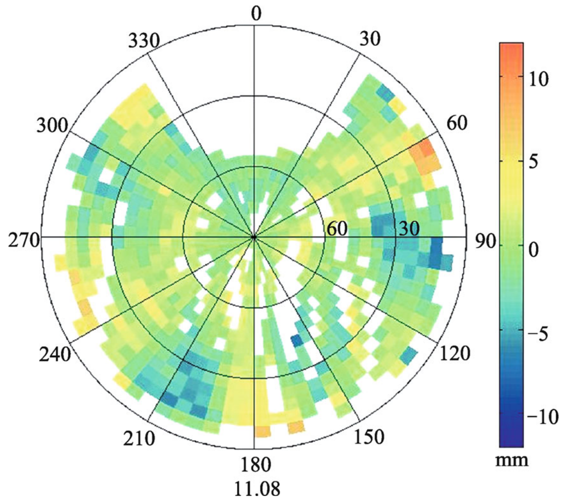

Fig. 4 Spatial distribution of multipath error on celestial hemisphere (Dong et al., 2014).

dynamic environment where the primary multipath is caused by the carrier body itself.

3.3 Phase center variation correction

Phase center variation (PCV) refers to the deviation of the instantaneous phase center of the antenna relative to its average phase center, which depends on the elevation (and azimuth) of the measured satellites. Both the transmitting and receiving antennas have PCV. Usually, PCV is several millimeters, and for some antennas up to several centimeters. Thus, it is a crucial error source and should be taken into account for high-precision GPS applications. For long baselines, PCV is difficult to eliminate or weaken using the difference method, and should be corrected by a model.

Measurement methods for the antenna PCV are divided into anechoic chamber measurements (Schupler et al., 1995) and field measurements (Wübbena et al., 1996; Mader, 1999; Bilich and Mader, 2010). The former method needs the construction of an anechoic chamber, which is costly, rendering it impractical for commercial use. In addition, although it is assumed there is no multipath effect in the anechoic environment, some research studies show that the pattern of the test antenna in an anechoic environment is different from in a field environment including multipaths (Rothacher et al., 1995; UNAVCO, 1995). Therefore, the field calibration is recognized as a more feasible method for calibrating PCV.

Field calibration methods include the SD method (Mader, 1999; Bilich and Mader, 2010) and DD method (Wübbena et al., 1996).

The calculation of PCV measurements with SD observations must rely on the clock synchronization technology, thus in this study we call these methods the MS-SD PCV measurement methods. Mader (1999) conducted relative PCV measurements through MS-SD phase observations. In this study, JPL D/M + crT is used as the reference antenna. The test antennas are located 5 m away at approximately the same height. A rubidium oscillator is used as an external frequency standard to eliminate the receiver clock error (Fig. 5). The root mean square repeatability of PCV obtained through correcting different antennas of the same type is on the order of several millimeters, which indicates that this method can be used for accurate PCV measurements. Clock synchronization technology can also be used for absolute PCV measurements, which are more accurate than relative PCV measurements. Bilich and Mader (2010) conducted absolute PCV measurements by forming the time difference of the MS-SD observations (TDSD for short). The calibration baseline is located in a large flat field with only a few reflecting objects in the far field (Fig. 6(a)). The referenced antenna was kept fixed while the test antenna was controlled by a two-axis robot that made it rotate automatically (Fig. 6(b)). The process of TDSD is: First, use the MS-SD operation to eliminate common errors such as the satellite clock, atmosphere, and receiver clock errors. Second, use the time-difference operation to eliminate multipath effects and the phase center of the reference antenna. Finally, the phase center offset and PCV of the test receiver are estimated with a two-stage least-squares solution based on the TDSD observations. A Septentrio AsteRx2eH MS-GNSS receiver was used in the comparison experiments on the Trimble Zephyr Geodetic 2 antennas (S/N 30212661 and 30212716) and Ashtech Geodetic III “Whopper” antennas (S/N 11885 and 11869) between the TDSD method and IGS measurement. The results show that the PCV values obtained using the TDSD method agree within 1 mm of the published IGS values.

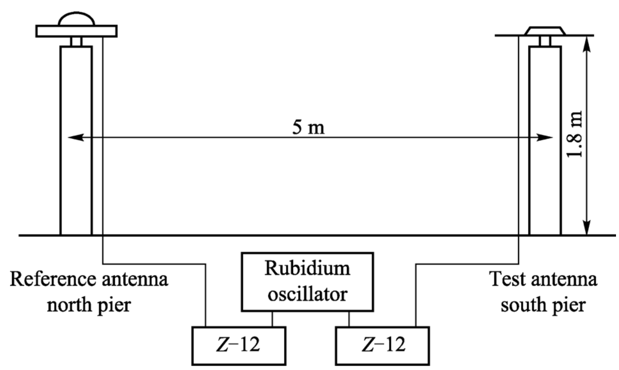

Fig. 5 Relative MS-SD PCV measurement experiment (Mader, 1999).

Wübbena et al. (1996) proposed a DD method for absolute PCV measurement. In this experiment, a reference antenna was fixed while the direction of the test antenna was variable, as in the TDSD method. There

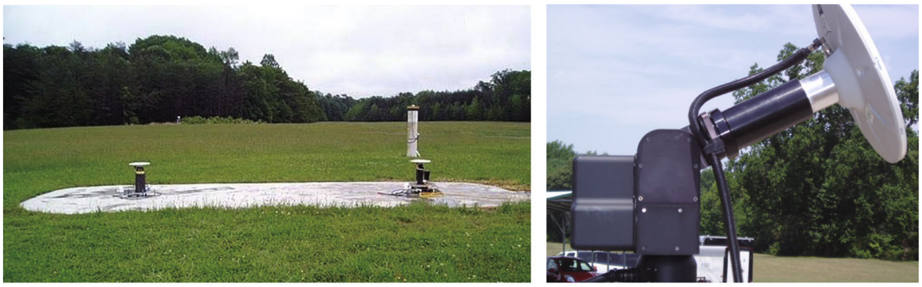

(a) (b)

Fig. 6 Absolute MS-SD PCV measurement experiment (Bilich and Mader, 2010). (a) The calibration baseline. (b) Two-axis robot used to move the test antenna.

are four steps in the DD absolute PCV measurement method. First, eliminate the multipath, PCV of the reference antenna, and the complete geometric information by building a mean sidereal day time difference. Second, eliminate the clock and atmospheric terms with DD. Third, estimate the DD PCV of the test antenna. Finally, calculate the PCV based on DD PCV.

Suppose that two epochs in a sidereal day interval are 1 and 2, and the common satellite is *i*. The final equation for SD PCV method can then be expressed as:

$$\Delta\nu_{12}^{i} = [\nu_2(a_2^i,z_2^i) - \nu_1(a_1^i,z_1^i)], \tag{10}$$

where *a* is the azimuth angle of the satellite and *z* is its elevation angle. Assume there is another satellite *j*, the equation of DD PCV solution is:

$$\nabla\Delta\nu_{12}^{ij} = [\nu_2(a_2^j,z_2^j) - \nu_1(a_1^j,z_1^j) - \nu_2(a_2^i,z_2^i) + \nu_1(a_1^i,z_1^i)]. \tag{11}$$

From the above two equations, it is obvious that the rank deficiency of the DD approach is more serious than that of the MS-SD approach. The rank deficiency of the MS-SD algorithm for PCV modeling is one. This rank deficiency is remedied by constraining the sum of the PCV solutions of all grids to be zero. Thus, the derived PCV plus PCO models (from an external source) represent the total antenna phase center variations at each grid. Meanwhile, the DD algorithm for PCV modeling has another one rank deficiency. Usually, we remove this extra rank deficiency by constraining the PCV solution at the central grid of the antenna to be zero. This constraint causes errors when the real PCV value at the central grid is not zero. Besides, the observation errors of the DD observables are larger than the errors of the MS-SD observables and are no longer independent at each epoch. Thus, the formal uncertainties of the PCV solutions of the DD algorithm are greater than those of the MS-SD algorithm by at least a factor of 1.4142. Thus, the MS-SD method can result in more precise PCV measurements than the DD method.

In summary, with the help of clock synchronization technology, we can obtain more precise PCV measurements. In addition, compared with previous experiments with external common clock equipment (Mader, 1999), the MS-GNSS receiver also increases the ease and feasibility of the experimental operation.

3.4 Ground-based carrier phase wind-up calibration

GPS signals are characterized by right-hand circle polarization, thus both transmitting and receiving antennas are right-hand circle-polarized antennas. When a satellite or receiving antenna rotates, an additive phase is generated. This phenomenon is called the phase wind-up effect (Tetewsky and Mullen, 1997). In particular, phase wind-up caused by the rotation of a satellite antenna is called space-based carrier phase wind-up (SPWU), whereas that caused by the rotation of a receiving antenna is called ground-based carrier phase wind-up (GPWU). Phase wind-up is unrelated to the position of the antenna carrier. However, it affects positioning accuracy, making it an important error source in precision positioning. SPWU is related to the angle between the connecting line of the satellite and the earth's center, and the connecting line of the satellite and the receiver. There are many studies on the influence, analytic expression, and modeling of SPWU (Wu et al., 1993; Kouba and Héroux, 2001). By contrast, few research studies have explored GPWU. Theoretical research indicates that, if the spin axis is aligned with the antenna boresight, the produced GPWU is independent of the satellite and is completely correlated with the receiver clock error. The GPWU effect is directly eliminated in DD observations and is completely absorbed by the receiver clock error parameters in routine SD and non-difference observations. Therefore, knowledge of the characteristics, effect, and potential use of the observed GPWU is still limited. Previous studies are mainly about the calibration of the GPWU effect in a non-difference solution. For example, to solve the problem of incompatibility in the conventional Precise Point Positioning (PPP) functional model caused by GPWU, Banville and Tang (2010) used two different clock parameters on phase observations and code observations to absorb the GPWU-based decoupled clocks model.

The MS-GNSS receiver provides an effective means for assessing the GPWU effect and its application because most of the other error sources have been eliminated. For a conventional receiver, GPWU will couple with the receiver clock error in SD and non-difference observations. Thus, it is difficult to obtain pure GPWU values in conventional cases. However, if a MS-GNSS receiver is used, the receiver clock error will be eliminated and the hidden GPWU value appears. Based on this property, Dong et al. (2015b) proposed a single antenna yaw angle determination (SAYD) method. The details of this follow. The linearized equation of MS-SD observations is:

$$\Delta\phi = \frac{1}{\lambda}(\Delta\rho_0^i + A\Delta X) + \Delta\varphi_{LB} + \Delta\varphi_{UPD} + \Delta\varphi_{GPWU} + \Delta N^i + \Delta\varepsilon, \tag{12}$$

where Δ is the MS-SD operator; i is the satellite index; $\Delta\rho_0^i$ is the initial value of the distance difference between the satellite and the two receiving antennas; A is the coefficient matrix of the baseline parameters; ΔX is the baseline parameters to be estimated; φ_{LB}, φ_{UPD}, and φ_{GPWU} are the line bias, UPD, and GPWU, respectively; N is the ambiguity parameters; λ is the wavelength of the carrier phase, and ε is the measurement of noise plus unmodeled errors. Because the coefficients of $\Delta\varphi_{LB}$, $\Delta\varphi_{UPD}$, and $\Delta\varphi_{GPWU}$ are the same, these parameters can be combined into one item and recorded as $\Delta\varphi_w$. Eq. (12) is then simplified as:

$$\Delta\phi = \frac{1}{\lambda}(\Delta\rho_0^i + A\Delta X) + \Delta\varphi_w + \Delta N^i + \Delta\varepsilon. \tag{13}$$

Here, $\Delta\varphi_{LB}$ and $\Delta\varphi_{UPD}$ are constants while $\Delta\varphi_{GPWU}$ is a stochastic parameter. If a proper perturbation value of $\Delta\varphi_w$ is assigned in Kalman filtering calculation, $\Delta\varphi_{GPWU}$ will be completely absorbed by $\Delta\varphi_w$. The epoch difference of $\Delta\varphi_w$ then represents the accumulated value of $\Delta\varphi_{GPWU}$ between these two epochs. An experiment was conducted to test the performance of SAYD. As shown in Fig. 7(a), one antenna was placed on a stationary tripod, and another on the turning table. The boresight of the antenna was consistent with its spin axis. Fig. 7(b) shows the changes in $\Delta\varphi_w$ over time. The horizontal axis refers to the epoch, and the vertical axis refers to the number of cycles. In this experiment, the antenna rotated for a total of 50 cycles, which coincided with the amount of the cumulative estimated MS-SD GPWU (about 50.47 cycles) (Fig. 7 (b)). The dispersion of the estimated yaw angle was 0.0579 cycles, and the mean error was 0.0094 cycles per cycle.

The MS-GNSS device makes it possible to observe and make use of the GPWU effect. The SAYD method, which is based on the MS-GNSS receivers, requires only one antenna and its solution accuracy is independent of the baseline length. Hence, the SAYD model demonstrates a potential advantage in the ultra-short baseline applications over the current GNSS yaw angle determination method using two antennas.

4 Summary and conclusions

This paper presented the MS-GNSS receivers which have been emerging rapidly in recent years. This type of receiver shows great advantages in high-precision positioning applications such as attitude determination, multipath effect elimination, PCV correction, and GPWU calibration:

1) For attitude determination, based on an MS-GNSS receiver, the MS-SD can eliminate both satellite and receiver clock errors simultaneously, which is equal to the conventional DD method. However, it has more observations and redundancy and appears less noisy. Its solutions show better repeatability and lower correlations among parameters. The MS-SD based ASA narrows the searching space of ambiguities and improves the efficiency and correctness of integer ambiguity resolution. Experiments under conditions of poor visibility also indicated that MS-GNSS receivers have the potential to improve the availability of signals.

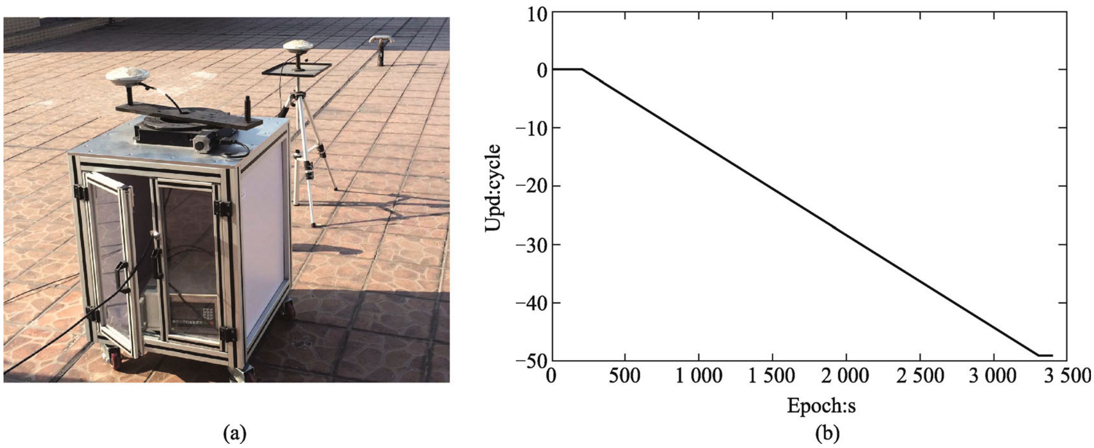

Fig. 7 Accuracy test experiment of SAYD with turning table. (a) Experiment setting. (b) Changes in φ_w over time.

2) For multipath effect mitigation, the MS-GNSS receiver obtains the SD residuals directly, therefore avoiding the transformation process from the DD residuals by adding constraints, thus making the ARTA method more precise. In addition, this receiver makes the look-up table method usable, and widens the application of multipath mitigation technology. Currently, the look-up table method is only for short baseline applications. Research on extending this method to PPP application will hopefully expand its scope of applications.

3) With the MS-GNSS receiver, the relative and absolute PCV can be measured directly, which can reduce the rank defect of the observation equation and improve the accuracy of measurement results. The MS-GNSS receiver can also simplify the operation process of PCV measurement.

4) The MS-GNSS receiver is able to separate the GWPU and receiver clock error, and provides an accurate means for assessing the GWPU effect. The SAYD method based on the measured GWPU has explored the potential of this receiver in yaw angle determination and demonstrates advantages in ultra-short baseline applications. At present, the SAYD method is based on the MS-GNSS receiver, and is feasible only when the distance between the two antennas is fairly short. Thus, solutions of wider applicability need to be further studied.

The development of the model and algorithm for the MS-GNSS receivers deserves further investigation. Improving the performance of this type of device will allow it to play a greater role in high-precision applications of positioning and attitude determination.

Acknowledgements This work is sponsored by the National Natural Science Foundation of China (Grant Nos. 61372086, 11373017, 41201380, 41171327, and 41201379), Foundation of Science and Technology Commission of Shanghai (Nos. 13511500300 and 15511101602), Open Research Funding of the Key Laboratory of Embedded System and Service Computing (No. 48505280) and Open Research Funding Program of KLGIS (No. KLGIS2014A02).

References

Alber C, Ware R, Rocken C, Braun J (2000). Obtaining single path phase delays from GPS double differences. Geophys Res Lett, 27(17): 2661–2664

Ashtech Inc. (1991). 3DF 24-Channel GPS measurement system. Houston: Ashtech Inc.

Banville S, Tang H (2010). Antenna rotation and its effects on kinematic Precise point positioning. In: Proceedings of ION GNSS-2010. Portland, OR, 2545–2552

Bilich A (2006). Improving the Precision and Accuracy of Geodetic GPS: Applications to Multipath and Seismology. Dissertation for Ph. D degree. Boulder: University of Colorado

Bilich A, Mader G L (2010). GNSS absolute antenna calibration at the National Geodetic Survey. In: Proceedings of ION GNSS-2010. Portland, OR, 1369–1377

Bock Y, Nikolaidis R, de Jonge P J, Bevis M (2000). Instantaneous geodetic positioning at medium distances with the Global Positioning System. J Geophys Res, 105(B12): 28223–28254

Cannon M E, Berry E, King M (1993). Testing a lightweight GPS/GIS terminal for sub-meter DGPS positioning. In: Proceedings of ION GPS-93. Salt Lake City, UT, 1011–1020

Cannon M E, Lachapelle G (1992). Analysis of a high-performance C/A code GPS receiver in kinematic mode. Navigation, 39(3): 285–300

Choi K, Bilich A, Larson K M, Axelrad P (2004). Modified sidereal filtering: implications for high-rate GPS positioning. Geophys Res Lett, 31(22): L22608

Cohen C E (1992). Attitude Determination Using GPS. Dissertation for Ph.D drgree. Stanford: Stanford University

Cohen C E, Parkinson B W (1991). Mitigating Multipath in GPS-Based Attitude Determination. In: 14th AAS Guidance and Control Conference. Keystone, Colo, 53–68

Dong D N, Chen W, Cai M M, Zhou F, Xia J C, Cheng M F, Yu C, Qiu S (2015a). Attitude determination solution for multi-antenna synchronized GNSS receiver. 201510015460.6.

Dong D N, Chen W, Yu C, Cai M M, Zhou F, Cheng Y N, Cheng M F, Lv J Y, Qiu S (2015b). Azimuth angle determination method from estimated ground-based carrier phase wind-up with multi-antenna synchronized GNSS receiver. 201510096274.X.

Dong D N, Zheng Z Q, Kuang L, Chen W, Wang Y F, Zeng Z, Song L, Zhou F, Cai M M, Zhang Q Q, Xia J C (2014). Multipath hemispherical model (MHM) for multipath mitigation. 201410310467.6.

Fenton P C, Falkenberg B, Ford T, Ng K, Van Dierendonck A J (1991). NoVatel's GPS receiver-the high performance OEM sensor of the future. In: Proceedings of ION GPS-91. Albuquerque, NM, 49–58

Fuhrmann T, Luo X G, KnöpflerA, Mayer M (2015). Generating statistically robust multipath stacking maps using congruent cells. GPS Solut, 19(1): 83–92

Ge L L, Han S W, Rizos C (2000). Multipath mitigation of continuous GPS measurements using an adaptive filter. GPS Solut, 4(2): 19–30

Ge M, Gendt G, Rothacher M, Shi C, Liu J (2008). Resolution of GPS carrier-phase ambiguities in Precise Point Positioning (PPP) with daily observations. J Geod, 82(7): 389–399

Genrich J, Bock Y (1992). Rapid resolution of crustal motion at short ranges with the Global Positioning System. J Geophys Res, 97(B3): 3261–3269

Hermann B R (1985). A Simulation of the navigation and orientation potential of the Ti-Agr. Mar Geod, 9(2): 133–143

Keong J, Lachapelle G (2000). Heading and pitch determination using GPS/GLONASS. GPS Solut, 3(3): 26–36

Kouba J, Héroux P (2001). Precise point positioning using IGS orbit and clock products. GPS Solut, 5(2): 12–28

Kruczynski L R, Li P C, Evans A G, Hermann B R (1989). Using GPS to determine vehicle attitude: USS Yorktown test results. In: Proceedings of ION GPS-89. Colorado Springs, 163–171

Larson K M, Bilich A, Axelrad P (2007). Improving the precision of high-rate GPS. J Geophys Res, 112(B5): B05422

Li Y, Zhang K, Roberts C, Murata M (2004). On-the-fly GPS-based attitude determination using single- and double-differenced carrier phase measurements. GPS Solut, 8(2): 93–102

Lu G, Lachapelle G, Cannon M E, Vogel B (1994). Performance analysis of a shipborne gyrocompass with a multi-antenna GPS system. In: Proceedings of IEEE PLANSc94. Las Vegas, 337–343

Mader G (1999). GPS antenna calibration at the national geodetic survey. GPS Solut, 3(1): 50–58

Nee R D J V (1992). The multipath estimating delay lock loop. In: Proceedings of IEEE 2nd Symposium on Spread Spectrum Techniques and Applications. Yokohama, 39–42

Ragheb A E, Clarke P J, Edwards S J (2007). GPS sidereal filtering: coordinate and carrier-phase-level strategies. J Geod, 81(5): 325–335

Rothacher M, Schaer S, Mervart L, Beutler G (1995). Determination of antenna phase center variations using GPS data. In: Proceedings of the IGS Workshop. Potsdam, Germany

Schupler B R, Clark T A, Allshouse R L (1995).Characterizations of GPS user antennas: reanalysis and new results. In: Beutler G et al., eds. GPS Trends in Precise Terrestrial, Airborne, and Spaceborne Applications. IAG Symposia, Vol.115. Boulder, CO, USA: Springer Verlag

Souza E M, Monico J F G (2004). Wavelet shrinkage: high frequency multipath reduction from GPS relative positioning. GPS Solut, 8(3): 152–159

Tetewsky A K, Mullen F E (1997). Carrier phase wrap-up induced by rotating GPS antennas. GPS World, 8(2): 51–57

Teunissen P J G (1995). The least-squares ambiguity decorrelation adjustment: a method for fast GPS integer ambiguity estimation. J Geod, 70(1-2): 65–82

Teunissen P J G, de Jonge P J, Tiberius C C J M (1997). The least-squares ambiguity decorrelation adjustment: its performance on short GPS baselines and short observation spans. J Geod, 71(10): 589–602

Townsend B, Fenton P (1994). A practical approach to the reduction of pseudorange multipath errors in A L1 GPS receiver. In: Proceedings of ION GPS-94, Salt Lake City, 143–148

UNAVCO (1995). Receiver and Antenna Test Report. University Navstar Consortium (UNAVCO) Academic Research Infrastructure (ARI), Boulder, Colorado

Van Dierendonck A J, Fenton P, Ford T (1992). Theory and performance of narrow correlator spacing in a GPS receiver. Navigation, 39(3): 265–283

Wilson G J, Tonnemacher J D (1992). A GPS attitude determination system. J Navig, 45(2): 192–204

Wu J, Wu S, Hajj G, Bertiger W, Lichten S (1993). Effects of antenna orientation on GPS carrier phase. Manuscr Geod, 18(2): 91–98

Wübbena G, Menge F, Schmitz M, Seeber G, Völksen C (1996). A new approach for field calibration of absolute antenna phase center variations. In: Proceedings of ION GPS-96. Kansas City, MO, 1205–1214

Ye S R, Chen D Z, Liu Y Y, Jiang P, Tang W M, Xia P F (2014). Carrier phase multipath mitigation for BeiDou navigation satellite system. GPS Solut, doi: 10.1007/s10291-014-0409-1

Young L, Meehan T (1988). GPS Multipath effect on code-using receiver. In: American Geophysical Union Meeting. Baltimore, MD, USA: 335–343

Zheng D W, Zhong P, Ding X L, Chen W (2005). Filtering GPS time series using a Vondrak filter and cross-validation. J Geod, 79(6 – 7): 363–369

Zhong P, Ding X L, Yuan L G, Xu Y L, Kwok K, Chen Y Q (2010). Sidereal filtering based on single differences for mitigating GPS multipath effects on short baselines. J Geod, 84(2): 145–158

Zhou F, Dong D N, Chen W, Cai M M (2015). Isolating fractional phase delays in single differences with common receiver clock. (Submitted to GPS solutions)

AUTHOR BIOGRAPHIES

Danan Dong received his PhD degree in Earth, Atmosphere, and Planetary Sciences from Massachusetts Institute of Technology in 1993. He is a professor of School of Information Science Technology at East China Normal University (ECNU) currently. Before joining the faculty at ECNU, he served as a senior researcher at Jet Propulsion Laboratory (JPL) for 18 years. His research interests include space geodesy and its geophysical applications, mass loading, crustal deformation, and terrestrial reference frame. He had involved in the development of several GNSS processing softwares GAMIT, QOCA, and PADS.

E-mail: dndong@cs.ecnu.edu.cn

Wen Chen received her PhD degree in geospatial information science from East China Normal University in 2010. She currently works as a lecturer of School of Information Science Technology at East China Normal University. Her major research interests include GNSS high-precision application and spatial analysis.

E-mail: wchen@sist.ecnu.edu.cn

Miaomiao Cai is currently a PhD student of School of Information Science Technology at East China Normal University. She holds an MS degree in ECNU. Her research areas include GNSS high-precision data processing and application of Lidar in deformation monitoring.

E-mail: mmcai@outlook.com

Feng Zhou is currently a PhD student of School of Information Science Technology at East China Normal University. He holds an MS degree in China University of Mining and Technology. His research areas include multi-GNSS precise positioning and ambiguity resolution, etc.

E-mail: zhoufecnu@163.com

Minghua Wang is currently a PhD student of College of Surveying and Geo-informatics at Tongji University. He holds an MS degree in Wuhan University. His research areas include GNSS multipath mitigation and its applications.

E-mail: wmhua@126.com

Chao Yu received his PhD degree in physical electronics from Shanghai Institute of Technical Physics of Chinese Academy of Sciences in 2005. He currently works as a senior engineer of School of Information Science Technology at East China Normal University. His major research interests include GNSS information processing and application.

E-mail: cyu@sist.ecnu.edu.cn

Zhengqi Zheng received his PhD degree in electronic science and technology from East China Normal University in 1998. He currently works as a professor of School of Information Science Technology at East China Normal University. His major research interests include GNSS application and indoor positioning.

E-mail: zqzheng@ee.ecnu.edu.cn

Yuanfei Wang received his PhD degree in geospatial information science from East China Normal University in 1998. He currently works as an associate professor of Key Lab of GIScience, Education Ministry of China at East China Normal University. His major research interests include GNSS and GIS application.

E-mail: y.f.wang@139.com